

Optimization of Textured Photonic Crystal Backside Reflector for Si Thin Film Solar Cells

Lirong Zeng, Peter Bermel, Yasha Yi, Ning-ning Feng, Bernard A. Alamariu, Ching-yin Hong, Xiaoman Duan, John Joannopoulos, and Lionel C. Kimerling
Massachusetts Institute of Technology, Cambridge, MA, 02139

ABSTRACT

In this work, a textured photonic crystal is used as a novel backside reflector for mono- and poly-crystalline Si thin film solar cells. The backside reflector has two components, a grating and a distributed Bragg reflector (DBR), both of which enhance light-trapping for the near-infrared region of crystalline silicon. Simulations based on the scattering matrix method were used to systematically optimize all the key parameters to achieve the highest efficiency for a given solar cell thickness. We found that the optimal length scales in the problem, namely the period of the grating, the etch depth of the grating, the Bragg wavelength of the DBR, and the anti-reflection coating thickness, all decrease linearly as the absorption layer becomes thinner. The optimal value for the dimensionless duty cycle of the grating is found to be around 0.5 for all cell thicknesses. For a 2 μm thick cell, the efficiency enhancement relative to a cell with unpatterned backside can be as high as 53% using the optimized design.

INTRODUCTION

Thin film solar cells (TFSC) are widely considered the most promising candidates for next generation photovoltaic applications because of their potentially much lower cost [1]. Currently, the efficiencies of TFSC, however, are very low due to their weak absorption of long wavelength photons. For indirect bandgap materials such as Si, this issue is especially severe. To tackle this problem, we invented a new light trapping scheme using a textured photonic crystal as a backside reflector which can enormously elongate the optical path length, resulting in nearly complete light absorption. It is composed of a reflection grating and a distributed Bragg reflector (DBR) [2]. When the DBR is constructed out of Si and SiO_2 , the stopband can be designed to cover the wavelength range in which crystalline Si exhibits weak absorption, approximately 800-1200 nm. A simple design for a grating targeted at a wavelength λ_g that will gain the most path length enhancement consists of alternating high and low index blocks of equal width (duty cycle=0.5), with an etch depth of $\lambda_g / 4n_{\text{Si}}$, and a period of $\lambda_g / n_{\text{Si}}$, where λ_g and n_{Si} are the bandgap wavelength and refractive index of Si, respectively. However, absorption over a wide wavelength range must be taken into account due to the broad span of solar flux [3]. This concept is quantified in the expression for the short circuit current density,

$$J_{sc} = \int_{\lambda_1}^{\lambda_2} qA(\lambda)s(\lambda)d\lambda \quad (1),$$

where λ_1 and λ_2 specify the wavelength range of absorption, q is the electron charge, $A(\lambda)$ is the absorption at a certain λ , and $s(\lambda)$ is the number of incident solar photons per unit area per second. Therefore, it is important to strategically place the strong absorption points by numerical simulation such that they also have high weight in order to achieve the highest efficiency for a given cell thickness.

Furthermore, as the active layer becomes thinner, photons with increasingly shorter wavelengths can not be sufficiently absorbed and need light trapping. For example, while a 50 μm thick film corresponds to the absorption length of photons with $\lambda=930$ nm, a 2 μm thick

active layer is just that of $\lambda=580$ nm photons [4]. Consequently, we expect that the optimal parameters for the grating and DBR, as well as the anti-reflection coating thickness should change with cell thickness.

DESIGN OPTIMIZATION BY SIMULATION

Scattering matrix method and optimization approach

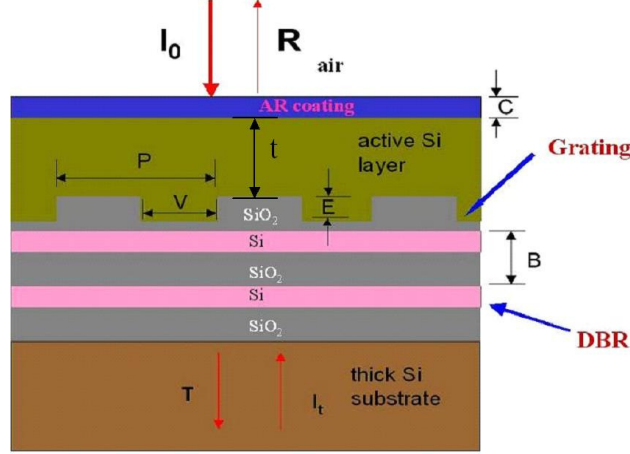


Figure 1. Schematic of a solar cell integrated with our textured photonic crystal backside reflector

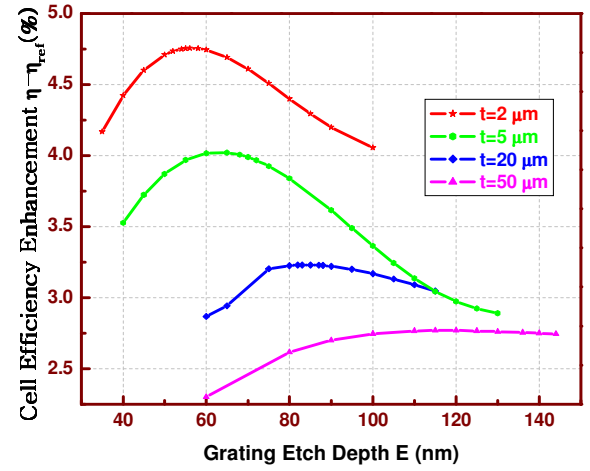


Figure 2. Grating etch depth optimization

The solar cell structure we simulate is shown in Figure 1. It is composed of a SiO₂ anti-reflection coating (ARC, thermal oxide is used for better surface passivation), active Si layer, grating and distributed Bragg reflector consisting of alternating layers of SiO₂ and Si films, and a 675 μm thick Si substrate that is treated as a semi-infinite medium. For cells with a given thickness t , the parameters to be optimized are: ARC thickness C , grating period P , etch depth E , duty cycle $F=V/P$, where V is the valley width, and Bragg wavelength λ_B of the DBR determined by the DBR period B . Our reference solar cell has a 120 nm thick ARC, and has no grating or DBR. Instead, it has a 0.5 μm thick SiO₂ layer between the active Si layer and the Si substrate for electrical isolation.

The optical constants of the active Si layer versus wavelengths are obtained from [4]. The refractive index of Si in DBR is set to be 3.5, and the index of SiO₂ in ARC, DBR and the isolation layer is set to be 1.46. For cells at a given thickness t , design parameters are optimized using a figure of merit which is the efficiency enhancement between cells with the textured back reflector and the reference cell.

Simulations based on the scattering matrix method [5] is used to calculate the solar cell efficiency and optimize the design. The approach is as follows: (1) Decompose the entire solar cell into uniform layers in the z direction; (2) Calculate the Fourier transform of the dielectric function of each layer; (3) Using the periodicity of the medium, transform the \mathbf{E} and \mathbf{H} fields into a Fourier series in each layer; (4) Use Maxwell's equation to derive the S-matrix, which relates fields in the adjacent layers at a given wavelength; (5) Compose the whole S-matrix; (6) Apply boundary conditions to get reflection R and transmission T (the incident intensity I_0 is known, and the reverse propagating light intensity in the substrate $I_t=0$), and obtain the

absorption $A=1-R-T$ for a given wavelength; (7) Repeat for all wavelengths that may be absorbed by our cell; and (8) Finally, use the absorption and solar spectra to obtain the solar cell efficiency by finding the maximum power point on the J-V curve. The current as a function of voltage can be written as the difference between the photon-induced current and the current induced by radiative recombination [6]:

$$J = \int_{\lambda_1}^{\lambda_2} qA(\lambda)s(\lambda)d\lambda - B \exp\left(\frac{eV - E_g}{kT}\right) \quad (2),$$

where B is a constant for a given cell. The maximum power point (J_m , V_m) is found by solving $d(JV)/dV=0$. J_{sc} is given in Eq. (1) and V_{oc} is found by setting $J=0$. The fill factor is

$$FF = \frac{J_m V_m}{J_{sc} V_{oc}}, \text{ and the solar cell efficiency is then}$$

$$\eta = \frac{J_{sc} V_{oc} FF}{P_{in}} \quad (3),$$

where $P_{in}=1000 \text{ W/m}^2$. It should be noted that no shadowing effect is considered here, and besides radiative recombination loss, photo-generated electrons and holes are assumed to be fully collected by the electrodes.

The optimization sequence used is: grating etch depth E; then grating period P; followed by DBR central wavelength λ_B ; ARC thickness; and grating duty cycle F. When optimizing a particular parameter, as in Figures 2 through 6, other parameters are held constant at approximately the values shown in Table 1. Then using this set of optimized parameters, we calculate cell efficiency enhancement, and repeat the cycle if necessary. Fifteen pairs of Si/SiO₂ serve as the DBR during the parameter optimization. Then, the number of quarter-wave pairs is reduced to eight to calculate the final efficiency enhancement, which corresponds to the number of pairs expected to be used in future experimental work. It is found that cell efficiency stays almost the same compared to 15-pair DBR. Four cell thicknesses are considered: 2, 5, 20 and 50 μm .

Parameter optimization

Figure 2 shows the grating etch depth vs. absolute solar cell efficiency enhancement relative to the reference cell for different cell thicknesses. The optimal etch depth decreases as the cell becomes thinner, changing from 115 nm for a 50 μm thick cell to the shallow 56nm for a 2 μm thick cell, which is less than half of the first value.

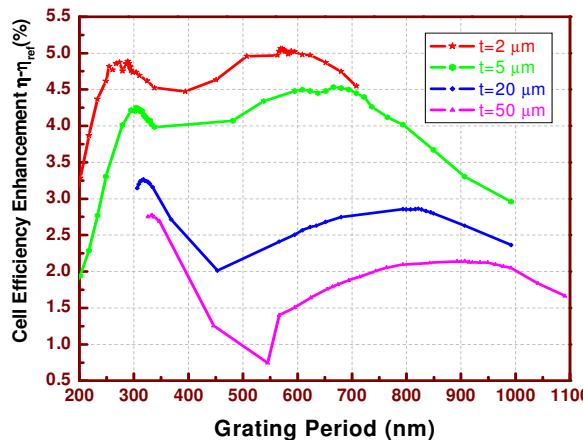


Figure 3. Grating period optimization

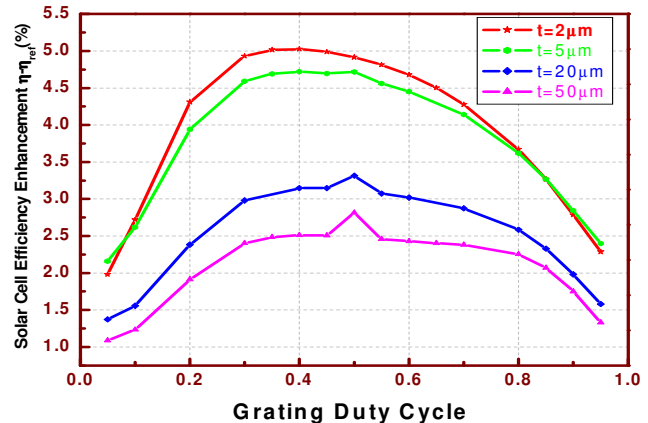


Figure 4. Grating duty cycle optimization

Figure 3 illustrates the optimization of the grating period. For different cell thickness t , all the curves have two maxima between 200 nm and 1100 nm. The first maximum, corresponding to first-order diffraction, is generally located around 300 nm, and the second maximum, corresponding to higher diffraction orders, varies from about 569 nm for $t=2\text{ }\mu\text{m}$ to 907 nm for $t=50\text{ }\mu\text{m}$. Both maxima decrease as cell thickness is decreased. For $t=50$ and $20\text{ }\mu\text{m}$, the first maxima have absolute efficiency obviously higher than the second ones ($>0.4\%$). As t decreases, the efficiency at the second maxima increases, and becomes slightly higher than the first one for $t=5$ and $2\text{ }\mu\text{m}$.

Figure 4 depicts the optimization of the grating duty cycle F . While both $t=50$ and $20\text{ }\mu\text{m}$ cells have sharp peaks at $F=0.5$, for $t=5\text{ }\mu\text{m}$, the cell efficiency is equal at both $F=0.4$ and 0.5 , and for $t=2\text{ }\mu\text{m}$, efficiency at $F=0.4$ is slightly higher than at $F=0.5$.

The central Bragg wavelength λ_B of the DBR is optimized in Figure 5. As cell thickness t decreases from $50\text{ }\mu\text{m}$ to $2\text{ }\mu\text{m}$, the center of the stop band decreases from 853 to 721 nm. The optimization of anti-reflection coating (ARC) thickness is shown in Figure 6. Again, as t decreases, ARC decreases from 108 nm to 92 nm, corresponding to a reduction of the reflection minimum ($\lambda=4tn_{\text{SiO}_2}$) from 631 nm to 537 nm.

The optimized parameters are summarized in Table 1. The trend of parameters variation and efficiency enhancement vs. cell thickness can be seen more vividly from Figures 7 and 8.

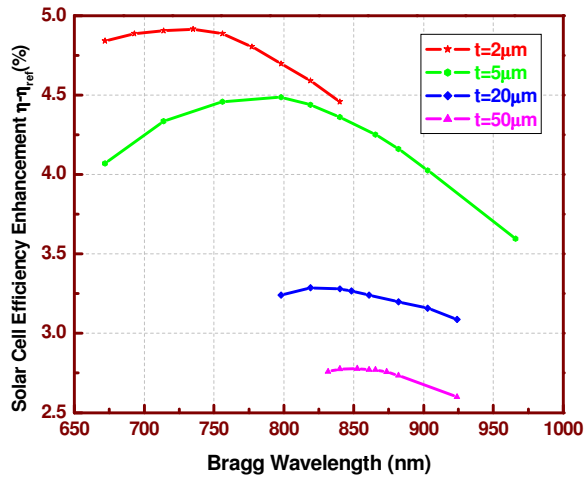


Figure 5. Bragg wavelength optimization

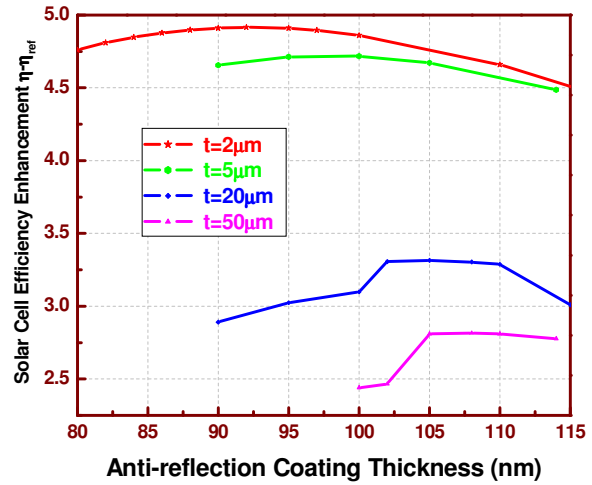


Figure 6. SiO₂ ARC thickness optimization

Table 1. Optimized solar cell design for different cell thicknesses

Solar cell thickness t (μm)	Grating etch depth (nm)	Grating period (nm)	Grating duty cycle	DBR Bragg wavelength (nm)	AR coating thickness (nm)	Optimized cell efficiency η_{opt} (%)	Reference cell efficiency η_{ref} (%)	$\frac{\eta_{\text{opt}} - \eta_{\text{ref}}}{\eta_{\text{ref}}}$ (%)
2	56	289	~ 0.5	721	92	14.5	9.5	52.6
5	65	304	~ 0.5	798	100	17.9	13.2	35.8
20	85	317	0.5	819	105	21.9	18.6	17.8
50	115	334	0.5	853	108	23.7	20.9	13.5

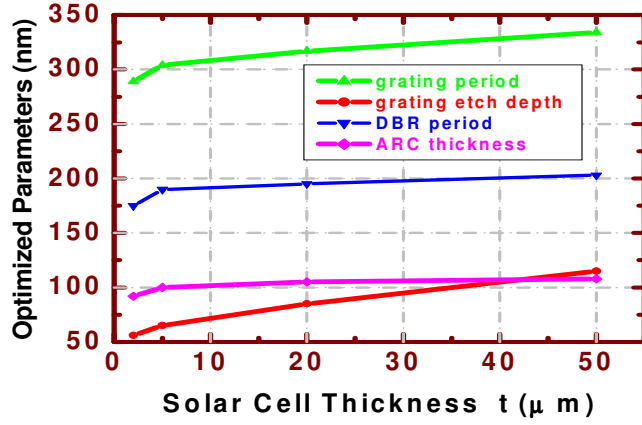


Figure 7. Optimized design parameters vs. cell thickness

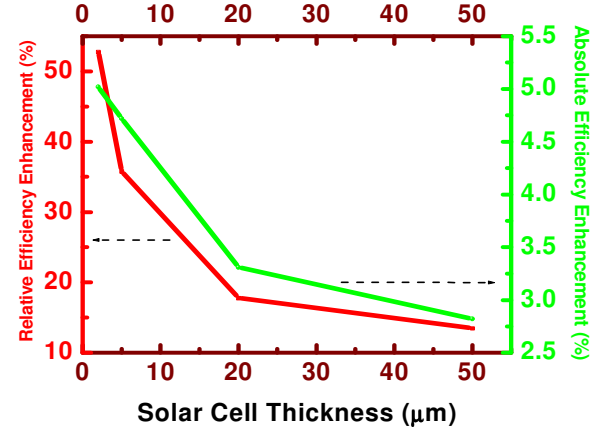


Figure 8. Efficiency enhancement vs. cell thickness

DISCUSSION

Choice of the optimized parameters will follow the following reasoning. The two maxima on each curve of Figure 3 should correspond to first and second order diffraction, respectively. It seems a good choice to use first order diffraction for all cell thicknesses. Table 1 shows clearly that the grating duty cycle remains almost constant at 0.5 for all cell thicknesses. This can be attributed to the fact that diffraction strength is proportional to the Fourier component of the grating period, which is maximized with an equal amount of high and low dielectric in the grating -- that corresponds to a duty cycle of 0.5. Also, it is clear from Figure 7 that as the active silicon layer becomes thinner, all the other optimized input parameters decrease monotonically. For $t \geq 5 \mu\text{m}$, the variation is linear, and for $t \leq 5 \mu\text{m}$, the slope is sharper. This behavior can be understood by noting that the absorption length of crystalline silicon monotonically increases with wavelength, which implies that the thinner the cell, the shorter the lower limit of the wavelength range that can benefit from light trapping. Figure 9 shows the absorption spectra of 50 and 5 μm thick solar cells. In the region of enhanced light trapping, resonant absorption peaks occur periodically. These modes are created by diffraction of the grating, and are confined within the silicon region by total internal reflection. Their spacing is inversely proportional to the cell thickness, so more densely spaced modes are seen in Fig. 9a, which is of a 50 μm -thick cell, than in 9b, which is of a 5 μm -thick cell. Compared to reference cells, when $t=50 \mu\text{m}$, significant absorption enhancement starts at $\lambda=800 \text{ nm}$, while when $t=5 \mu\text{m}$, strong enhancement starts at $\lambda=550 \text{ nm}$. Once one has determined that light trapping should start from shorter wavelength, it is clear that because of the scale-invariance of Maxwell's equations, all the back-reflector parameters should decrease accordingly.

For example, from the grating equation $m\lambda = p(\sin \alpha + \sin \beta)$, it can be seen that in order to achieve the same diffraction angle β for the same incidence angle α and diffraction order m , the period p should be proportional to the diffraction wavelength λ . The etch depth decrease can be predicted by writing a simple expression for the cancellation of the 0th order reflection,

$$E = \frac{\lambda}{4(n_{\text{Si}} - n_{\text{SiO}_2})}$$
 The DBR central wavelength decreases because the stopband needs to cover shorter wavelengths in thinner cells. Finally, the ARC thickness decreases, because it is

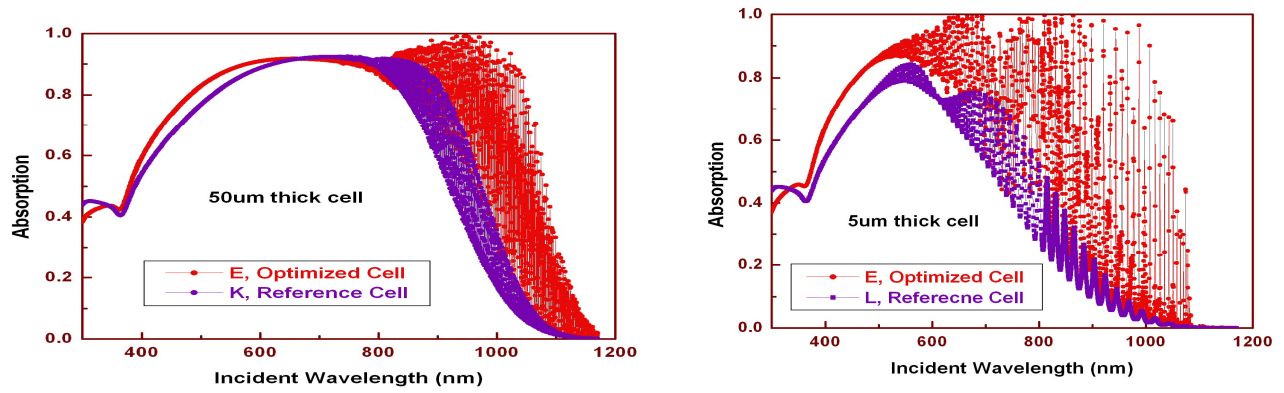


Figure 9. Absorption spectra of solar cells with different thicknesses
(a) 50 μm thick; (b) 5 μm thick.

beneficial to preferentially admit photons into the cell that can be effectively absorbed.

It is also obvious from Figure 8 that as the cell becomes thinner, both the absolute and relative efficiency enhancements increase sharply. For a 2 μm thick cell, the relative efficiency enhancement can be as high as 53%.

CONCLUSIONS

All the parameters of textured photonic crystal backside reflector are systematically optimized for solar cell efficiency by the scattering matrix method. Except for the grating duty cycle which remains almost constant at 0.5, grating etch depth, period, DBR central wavelength, and anti-reflection layer thickness all decrease as cell becomes thinner. This is explained by the blue shift of the lower limit of the wavelength range that needs light trapping when the cell thickness decreases. The optimized back reflector design can be readily applied to monocrystalline and polycrystalline Si thin film solar cells.

ACKNOWLEDGEMENTS

The authors would like to thank Jifeng Liu for helpful discussions.

REFERENCES

1. Y. Hamakawa (Ed.), Thin-Film Solar Cells, Next generation Photovoltaics and Its Applications, Springer, Berlin; New York, 2004.
2. L. Zeng, Y. Yi, C. Hong, B. A. Alamariu, J. Liu, N. Feng, X. Duan, and L. C. Kimerling, *Appl Phys. Lett.*, **89**, 111111 (2006).
3. ASTM G173-03, Standard Tables for Reference Solar Spectral Irradiances: Direct Normal and Hemispherical on 37 degree Tilted Surface (ASTM International, West Conshohocken, Pennsylvania, 2005).
4. C. Herzinger, B. Johs, W. McGahan, J. Woollam, and W. Paulson, *J. Appl. Phys.* **83**, 3323 (1998).
5. M. Auslender and S. Hava, *Optics Letters*, **21**, 1765 (1996); D. Whittaker and I. Culshaw, *Phys Rev. B* **60**, 2610 (1999).
6. C. H. Henry, *J. Appl. Phys.*, **51**, 4494 (1980).